

# EBSD Observations of the Evolution of Crystallographic Orientation During In-Situ Deformation\*

## Introduction

A fully annealed medium carbon structural steel tensile specimen was prepared by mechanical polishing followed by a 3% Nital etch. The specimen was positioned in the tensile stage grips and given a 20° pre-tilt. The SEM stage was tilted 50° resulting in a total tilt of 70°. The tensile test was paused after every 1  $\mu\text{m}$  of elongation to perform an OIM scan. In this technical note, we discuss the characterization of orientation gradients that develop within individual grains during in-situ tensile deformation.

## Orientation Gradient

OIM Analysis™ has several tools for characterizing the changes in orientation that occur during the plastic deformation of crystalline materials (see [2] for a review of these tools). One metric is Grain Reference Orientation Deviation or GROD. GROD maps show the orientation heterogeneities that evolve during deformation. Each pixel in the grain is colored based on the misorientation of the point relative to a reference orientation for the grain to which the pixel belongs. Part of the motivation for this work was to explore the several different approaches that have been proposed [3-5] for the choice of reference orientation and are summarized in Table 1.

With the in-situ experiment, we have orientation data at successive strain steps during deformation and can thus calculate another GROD variant where the reference orientation is the orientation of the grain prior to deformation -  $\text{GROD}_0$ .

The set of GROD maps for the EBSD data at 10% strain are shown (Figure 1). If we focus on the large grain at the center of the maps, then, except for the  $\text{GROD}_0$  map, the maps essentially show the fragmentation of the grain in terms of lattice rotation necessary to maintain compatibility with the neighboring grains - i.e. the Sachs iso-stress model [6]. The  $\text{GROD}_0$  map shows much less variation in misorientation indicative of a result more like the Taylor iso-strain model [6] where the grain rotates as a whole (Figure 2).

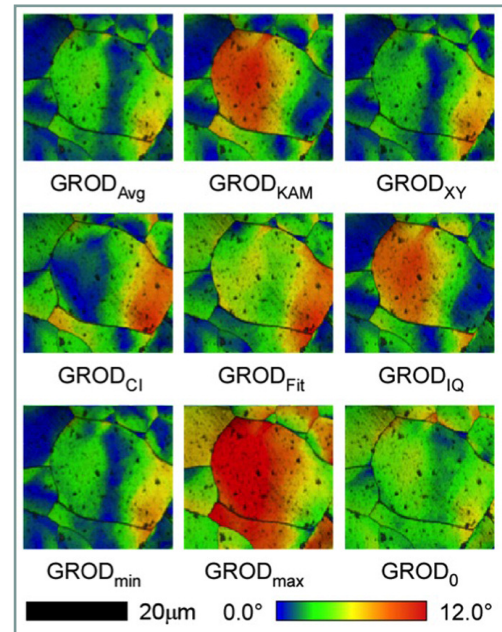


Figure 1. Set of GROD maps for the EBSD data at 10% strain.

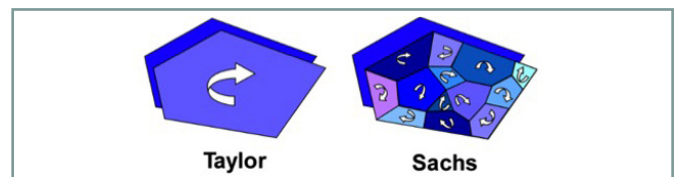


Figure 2. Illustration of the local changes in orientation that occur with deformation according to the Taylor iso-strain model (left) and Sachs iso-stress model (right).

GROD Variant	Reference Orientation Selection Criterion
$\text{GROD}_{\text{Avg}}$	Average orientation of all points in grain [2]
$\text{GROD}_{\text{KAM}}$	Orientation of point in grain producing the minimum KAM [2]
$\text{GROD}_{\text{XY}}$	Orientation of point in grain nearest the centroid of grain
$\text{GROD}_{\text{IQ}}$	Orientation of point in grain with the highest IQ [3, 4]
$\text{GROD}_{\text{CI}}$	Orientation of point in grain with the highest CI [4]
$\text{GROD}_{\text{Fit}}$	Orientation of point in grain with the smallest Fit [4]
$\text{GROD}_{\text{min}}$	Orientation of point in grain producing the minimum overall average GROD value [5]
$\text{GROD}_{\text{max}}$	Orientation of point in grain producing the maximum overall average GROD value [5]

Table 1. Different approaches that have been proposed for the choice of reference orientation.

\*This is a summary of a paper published in JOM[1].

Often, it is assumed that the low misorientation regions (blue in the color scale used) represent non-deformed material. This is the rationale for using the points with the minimum KAM, maximum CI, maximum IQ, minimum Fit and minimum overall GROD as reference orientations as such criteria would generally be assumed to correspond with non-strained material. However, while there is some correlation between the maps associated with some of these parameters, they are not at all consistent, suggesting that the assumption that the blue regions in these maps represent stationary material is invalid. This was also confirmed with KAM maps.

## Grain Boundaries

The grain boundary misorientation, in terms of both axis and angle, changes significantly between 0% and 10% strain as can be seen in Figure 3. The change in the axis can be seen by comparing the location of the misorientation axes in both the inverse pole figures (showing the orientation of the misorientation axis in crystal space) and the pole figures (showing the misorientation axis in sample space) before and after deformation. The location and spread of misorientation at 0% strain is indicated in the inverse pole figure and pole figure after 10% strain by black circles. The change in the misorientation angle is evident in the chart below the pole figures and maps.

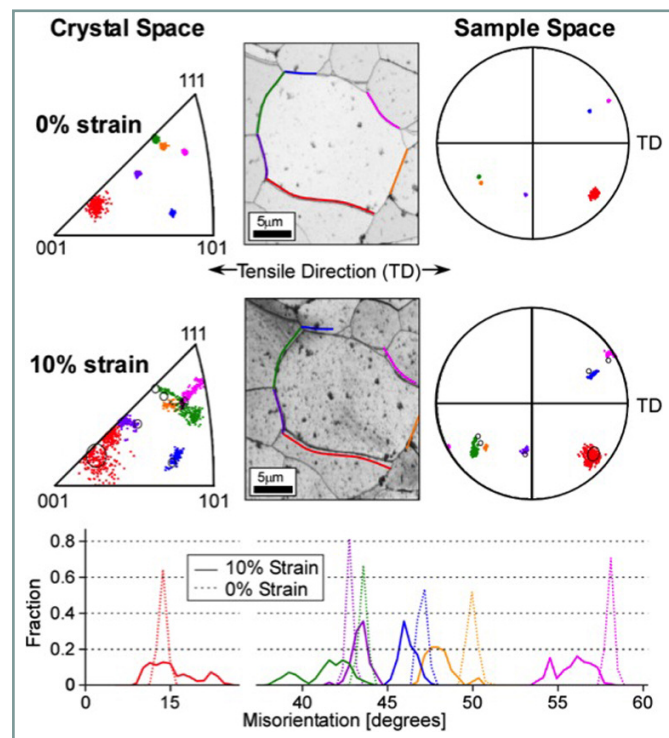


Figure 3. Inverse pole figures, maps, and pole figures showing changes between 0% and 10% strain (top). Chart showing change in misorientation angle (bottom).

The deformation initiates a rotation of the crystallographic lattice within each grain. This not only leads to a change in misorientation but also to an increase in the spread in misorientation along the grain. The need to reach compatibility between the lattices of two neighboring grains leads to the spread in misorientation. These observations are consistent with observations of dislocation accumulation at grain boundaries.

## Conclusions

- The overall change in orientation shown in the  $GROD_0$  map is reflective of the overall Taylor-like rotations of the individual grains in the polycrystal, whereas the variances in misorientations in the other GROD maps are reflective of grain fragmentation ala the Sachs model of deformation.
- A comparison of the  $GROD_0$  map with the other GROD variants shows that it is incorrect to assume that regions of low angle misorientation (blue in the color scheme used) in conventional GROD maps represent material that is stationary and that the high angle areas represent material that is rotating around or away from neighboring low angle misorientation areas.
- The misorientation at grain boundaries changes both in axis and angle with increasing deformation.

## References

1. SI Wright, S Suzuki & MM Nowell, *JOM* **68**: 2730 (2016).
2. SI Wright, MM Nowell & DP Field, *Microsc. Microanal.* **17**: 316 (2011).
3. T Zhang, DM Collins, FP Dunne & BA Shollock, *Acta Mater.* **80**: 25 (2014).
4. Y Mikami, K Oda, M Kamaya & M Mochizuki, *Mater. Sci. Eng.* **647**: 256 (2015).
5. V Khademi, T Bieler & C Boehlert in Advanced Characterization Techniques for Quantifying and Modeling Deformation at TMS 2016. Nashville, Tennessee. (2016).
6. For a comparison of the Sachs and Taylor models see Professor Anthony Rollett's lecture on polycrystal plasticity: [http://pajarito.materials.cmu.edu/rollett/27750/L11-PolyXtal\\_plast-Aniso3-25Feb16.pdf](http://pajarito.materials.cmu.edu/rollett/27750/L11-PolyXtal_plast-Aniso3-25Feb16.pdf).